

Electronic Supplementary Information

Immobilization of Cationic Dye on photoluminescent hydroxyapatite particles through a citric acid bonding layer

Daichi Noda ^{1,2}, Wanyu Shi ^{1,2}, Aiga Yamada ¹,
Zizhen Liu ^{1,2} and Motohiro Tagaya ^{*, 1}

¹. *Department of Materials Science and Technology, Nagaoka University of Technology,
1603-1 Kamitomioka, Nagaoka, Niigata 940-2188, Japan*

². *Research Fellow of the Japan Society for the Promotion of Science (DC),
5-3-1 Koji-machi, Chiyoda-ku, Tokyo 102-0083, Japan.*

*** Author to whom correspondence should be addressed:**

Tel: +81-258-47-9345; Fax: +81-258-47-9300, E-mail: tagaya@mst.nagaokaut.ac.jp

Figure S1

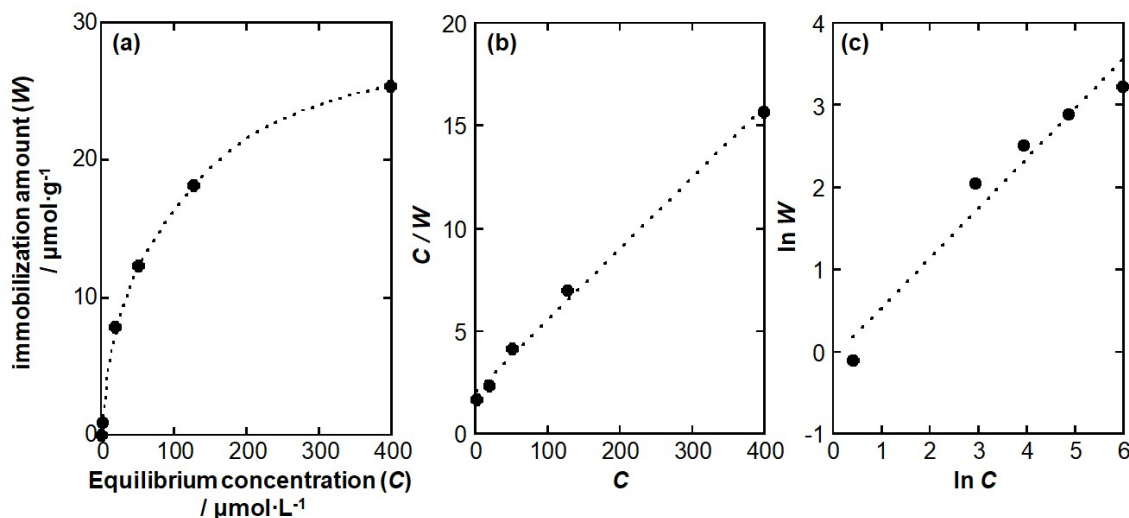


Figure S1. (a) Adsorption isotherm of TMPyP on CEHAp, and the linear regression fitting plots based on (b) Langmuir and (c) Freundlich equation types ($R^2 = 0.9944$ and 0.9494). Specifically, to evaluate the adsorption state, the adsorption isotherms were prepared. In the case of monolayer adsorption on the nanoparticle surfaces, the Langmuir adsorption equation obtained from the isotherm is shown as the equation (S1).^{S1}

$$\frac{C}{W} = \frac{1}{W_{\max}}C + \frac{1}{W_{\max} * K_{eq}} \quad (\text{S1})$$

Here, W is the adsorption amount ($\mu\text{mol/g}$), C is the equilibrium concentration ($\mu\text{mol/L}$), W_{\max} is the maximum adsorption amount, and K_{eq} is the adsorption equilibrium constant (g/L). Whereas, in the case of non-uniform adsorption on the nanoparticle surfaces, the Freundlich adsorption equation obtained from the isotherm is shown as the following equation (S2).^{S2}

$$\ln W = \ln K_F + (1/n)\ln C \quad (\text{S2})$$

Here, K_F and n are the Freundlich coefficient and adsorption constant, respectively. For the Langmuir equation, analysis was performed by plotting C and C/W on the horizontal and vertical axes, respectively. The analysis for the Freundlich equation was by plotting $\ln C$ and $\ln W$ on the horizontal and vertical axes, respectively.

References

- S1 I. Langmuir, *J. Am. Chem. Soc.*, 1918, **40**, 1361–1403.
S2 H. Freundlich and G. Losev, *Zeitschrift für Phys. Chemie*, 1907, **59U**, 284–312.

Figure S2

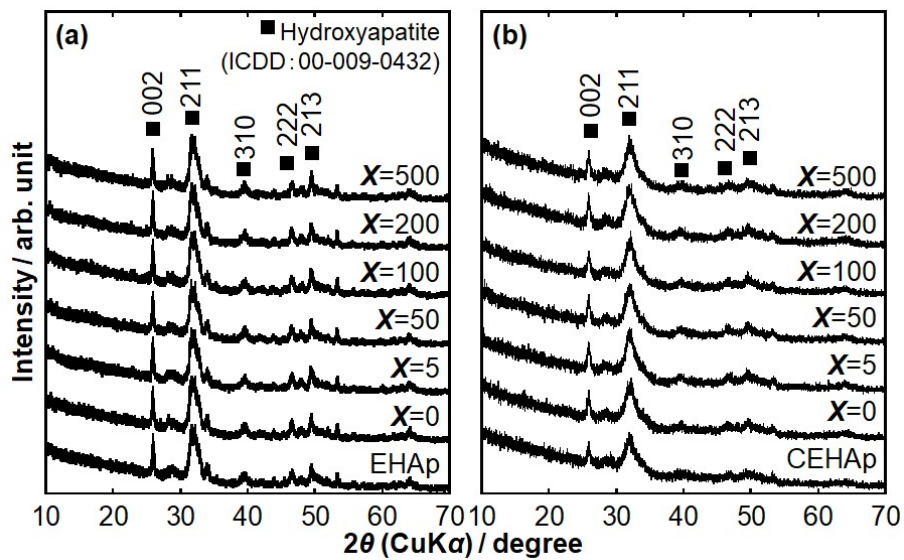


Figure S2. XRD patterns of (a) TX-EHAp and (b) TX-CEHAp, and all the patterns can be attributed to hydroxyapatite (ICDD No. 00-009-0432).

Figure S3

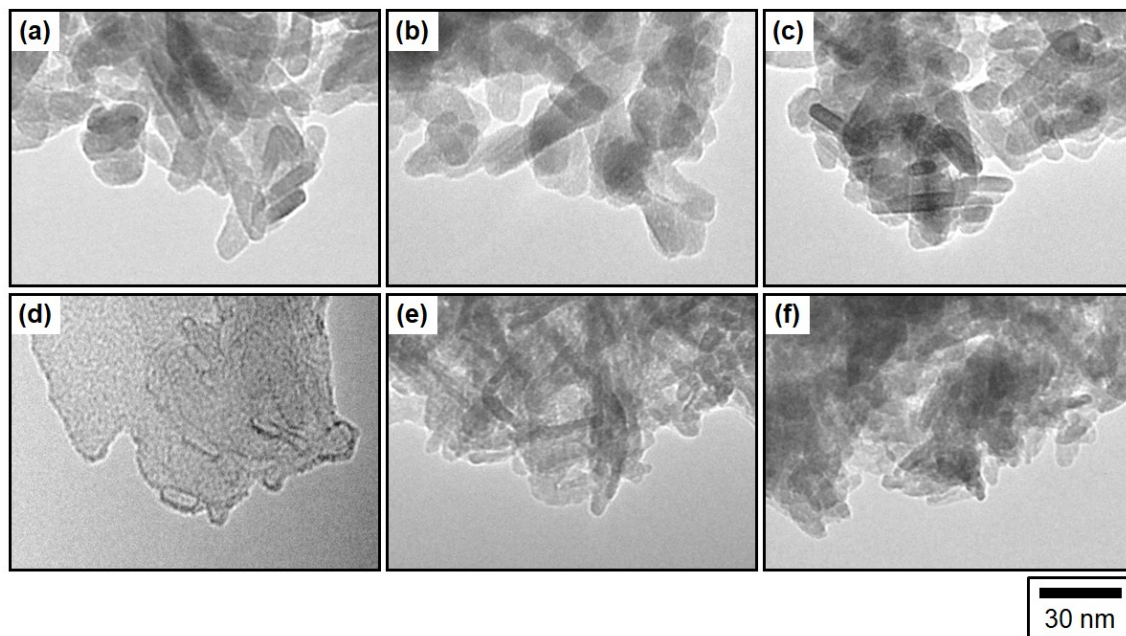


Figure S3. TEM images of (a) EHAp, (b) T50-EHAp, (c) T500-EHAp, (d) CEHAp, (e) T50-CEHAp and (f) T500-CEHAp.

Figure S4

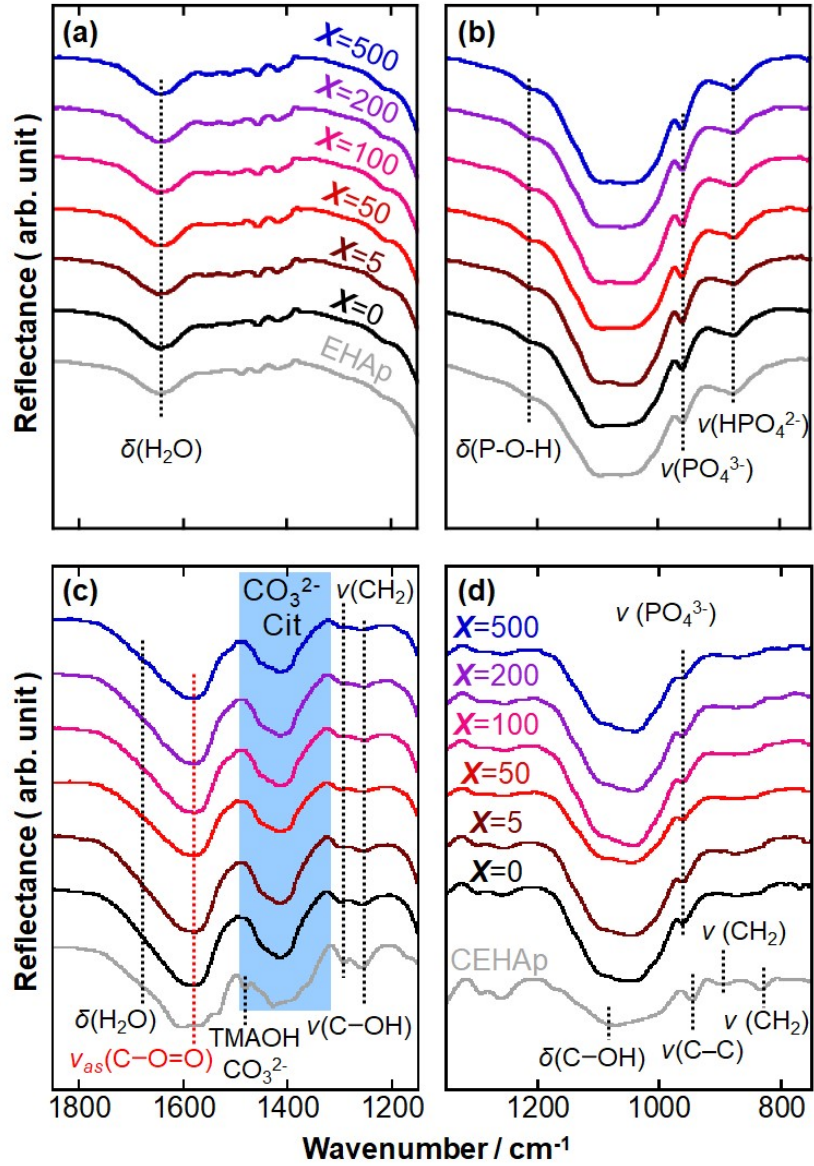


Figure S4. Characteristic absorption bands of (a, c) carbonate and (b, d) phosphate ions of (a, b) TX-EHAp and (c, d) TX-CEHAp in the FT-IR spectra.

Figure S5

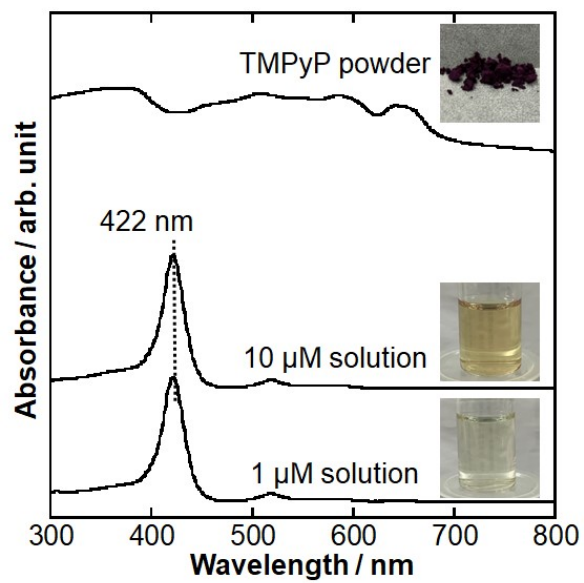
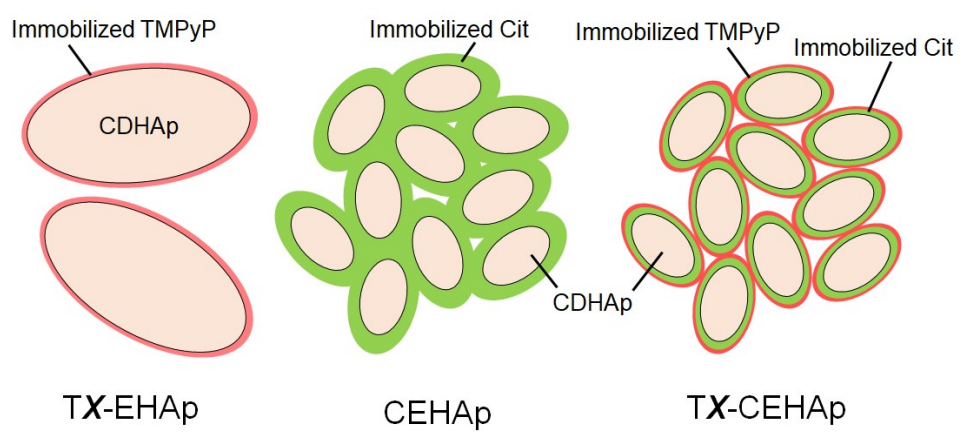


Figure S5. UV-Vis absorption spectra of the TMPyP powder and solutions (conc. 1 and 10 μM).

Scheme S1



Scheme S1. Illustration of the particle states of TX-EHAp, CEHAp and TX-CEHAp.

Figure S6

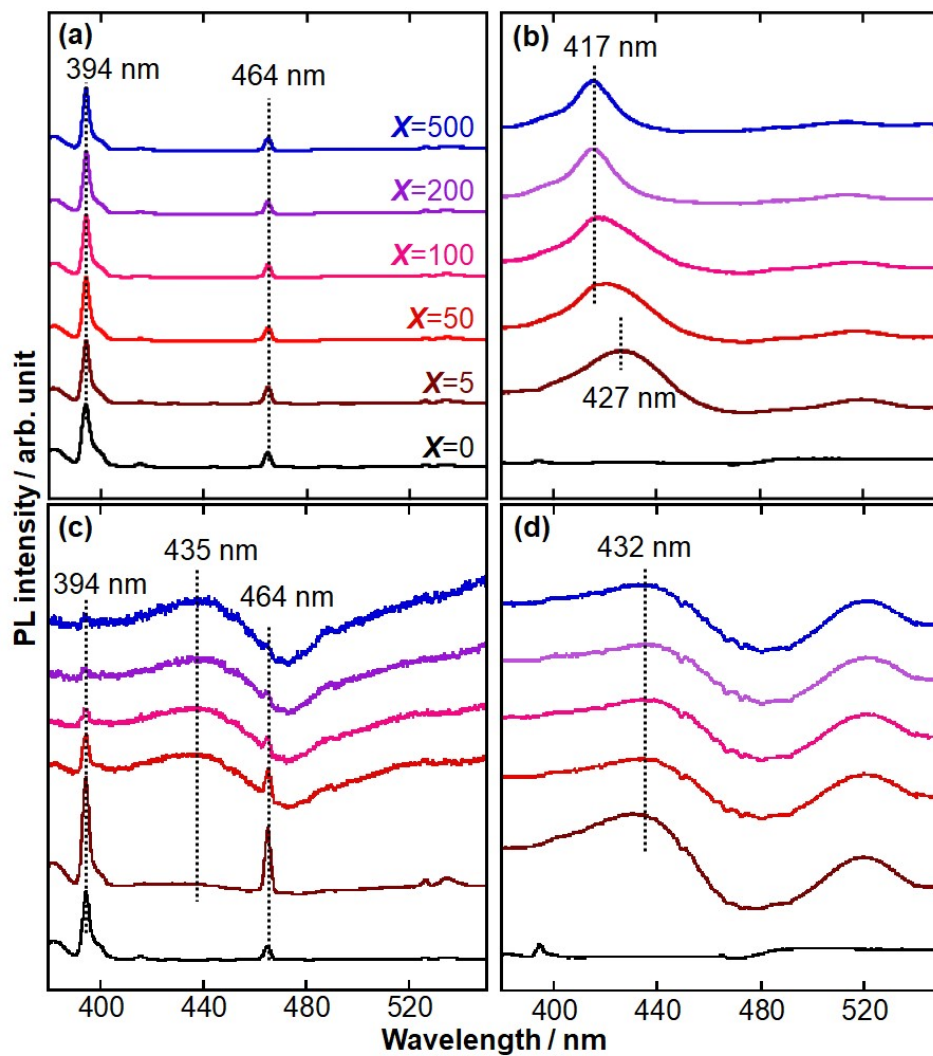


Figure S6. Excitation spectra of (a, b) TX-EHAp and (c, d) TX-CEHAp for the detected PL wavelengths at (a, c) 616 and (b, d) 720 nm.

Figure S7

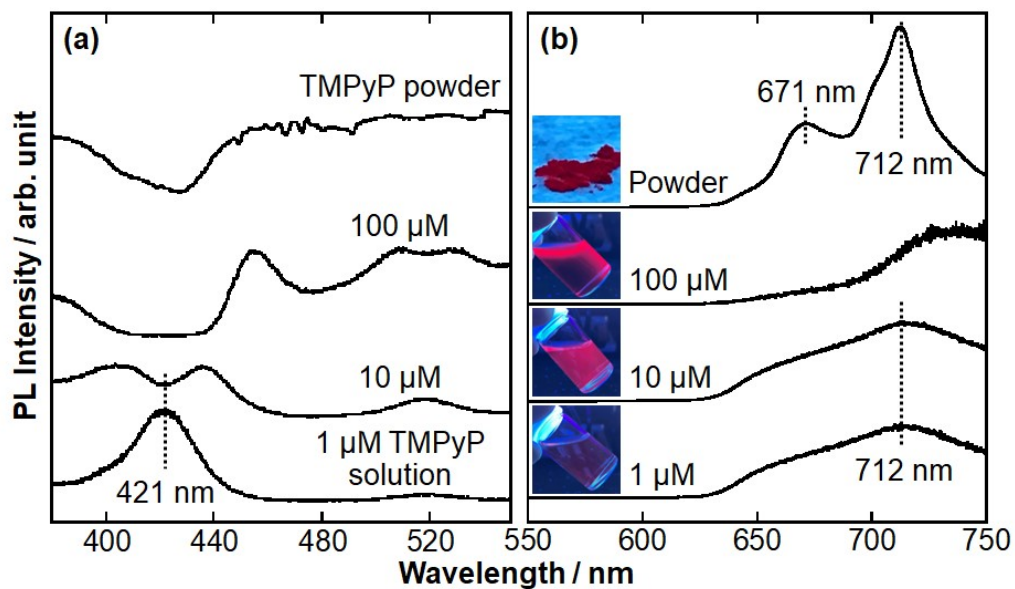


Figure S7. (a) Excitation and (b) PL spectra of the TMPyP powder and solutions (conc. 1, 10, 100 μM) at the detected PL and excitation wavelengths of 720 and 420 nm, respectively.

Figure S8

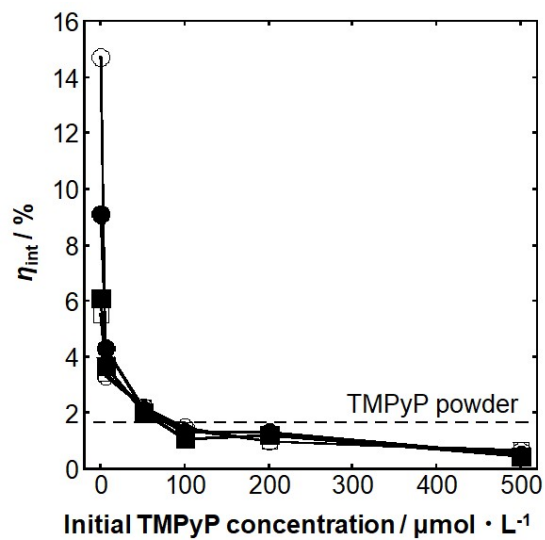


Figure S8. η_{int} value changes of (●, ■) TX-EHAp and (○, □) TX-CEHAp at the detected excitation wavelengths of (○, ●) 394 and (□, ■) 427 nm with the initial TMPyP concentration.

Figure S9

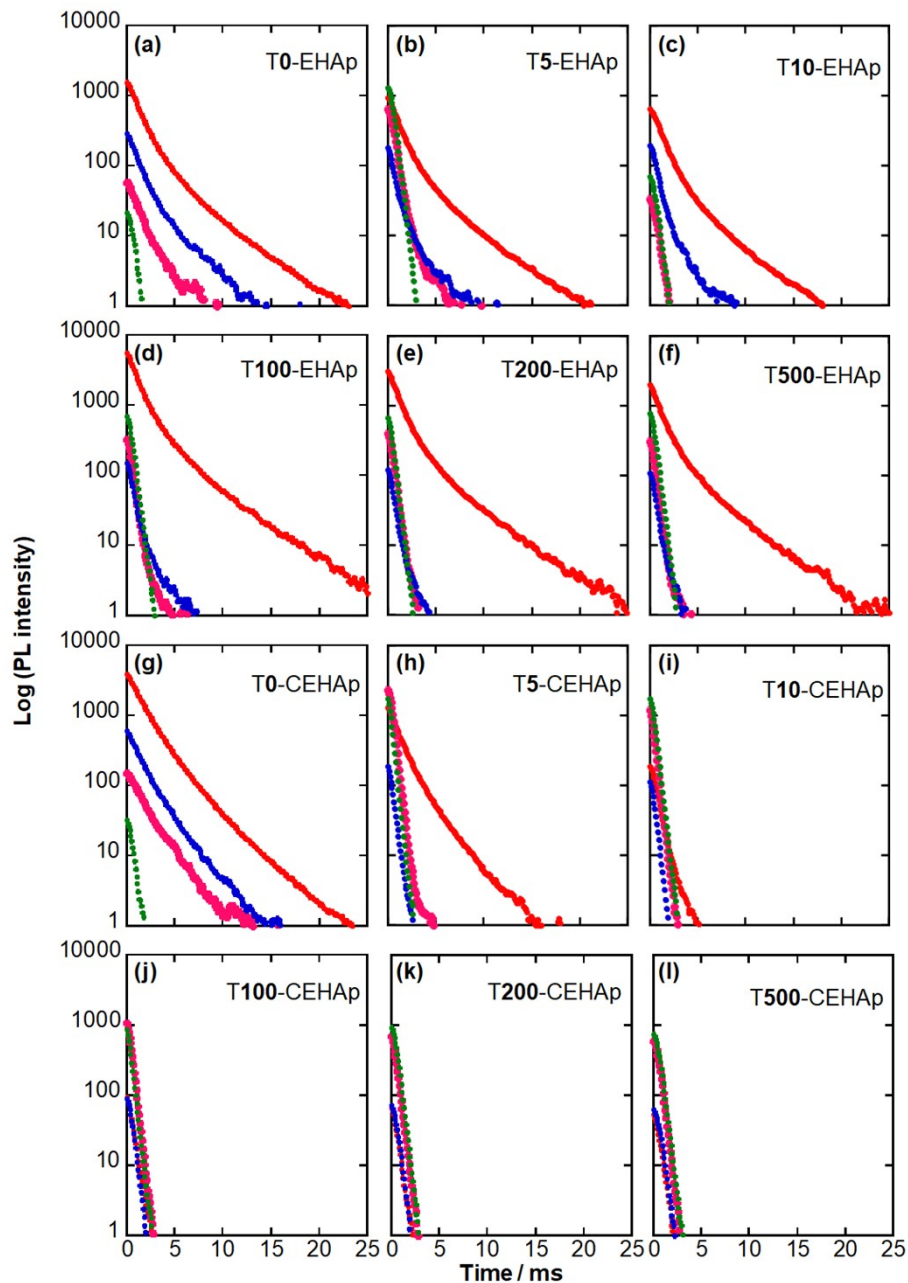


Figure S9. PL intensity decay plots of (a-f) TX-EHAp and (g-l) TX-CEHAp ($X=0, 5, 50, 100, 200, 500$), and the excitation/PL wavelengths for the plots were 394/616 nm (red-color), 394/720 nm (pink-color), 427/616 nm (blue-color) and 427/720 nm (green-color), respectively.

Figure S10

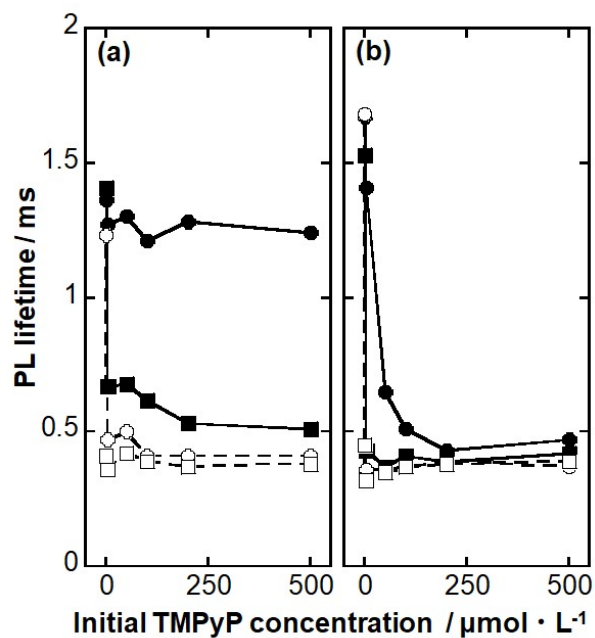


Figure S10. PL lifetime changes of (a) TX-EHAp and (b) TX-CEHAp with the initial TMPyP concentration. Here, the excitation/PL wavelengths for the plots were (●) 394/616 nm, (■) 427/616 nm, (○) 394/720 nm and (□) 427/720 nm.